OPTICAL HYPERFINE STRUCTURE IN CdII

A Thesis

Presented to

the Faculty of Graduate Studies

and Research

The University of Manitoba

In Partial Fulfillment

of the Requirements for the Degree

Master of Science

---

by

John Beattie Sutherland

October 1957

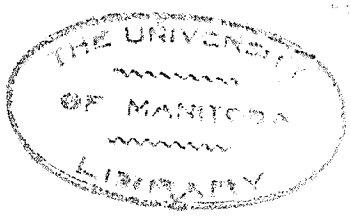

ABSTRACT:

In this work, the validity of calculating the Fermi-Segre factor $(1 - \frac{d\sigma}{dn})$ by the method of Crawford and Schawlow has been investigated. This factor arises in the Goudsmit Fermi-Segre formula for calculation of the nuclear magnetic moment. Measurements of the hyperfine structure of the 5s level of the Cd II spectrum have been obtained from the resonance lines (λ 2144 and λ 2265) $5s^2S_{1/2}$ - $5p^2P_{3/2,1/2}$, and these measurements used in calculating the nuclear magnetic moment of the cadmium nucleus from the Goudsmit Fermi-Segre formula. This value has been found to be $\mu = -0.60 \pm 0.03$ nuclear magnetors. This compares with the corrected values as calculated from the 6s level and with the value obtained by nuclear induction method. This consistency of the results supports the calculation of the Fermi-Segre factor by the method of Crawford and Schawlow.

There is a short description of the operation of an evaporator for use in coating the quartz plates of a Fabry-Perot Interferometer to obtain the resolving power required for the experiment.

TABLE OF CONTENTS

I. INTRODUCTION

When certain lines which occur in atomic spectra are examined with high resolution instruments, they are found to be composed of several components. This structure is known as hyperfine structure (hfs). The magnitudes of the observed hfs vary widely, the largest being found in the heavy elements. For an individual element, the largest structures are in energy levels involving a single unpaired s-electron with small principal quantum numbers.

Two types of hfs have been recognized. The first is due to the presence of two or more isotopes in the element being studied and is known as isotope shift. For the lighter elements, I.S. can be explained on the basis of the different nuclear masses of the isotopes. This mass effect can in turn be separated into the normal mass effect and the specific mass effect. The normal mass effect, in which the mass of the electron is replaced by the reduced mass of the electron, completely explains the I.S. for one-electron hydrogenic spectra. The effect is easy to calculate. Normal mass effect must be taken into account for every atomic energy level, although it decreases rapidly for an increase in the atomic weight. The specific mass effect is caused by the interaction of two or more electrons. The calculation of the S.M.E. involves the numerical evaluation of integrals of the same form as those that arise in intensity calculations. The calculations are involved and only a few have been undertaken. (For example see Vinti 1938). The S.M.E. also decreases with increasing atomic weight since for heavier elements the shifts have been completely explained by the field or volume effect. (Crawford and Schawlow, 1949).

The field effect is due to the departure from the Coulomb potential of the electrical potential experienced by the electron within the volume of the nucleus. Since the two isotopes have differing nuclear radii, the binding of the electron to the nucleus will be larger for the isotope of the smaller radius. This results in a differential shift of the energy levels of the various isotopes, and is observed as isotope shift.

The second type of hfs can be observed in the spectrum of an element having only one isotope (eg. Bi) and therefore cannot be explained on the basis of isotope shift. The explanation was first given by Pauli who postulated a spin angular momentum and an associated magnetic moment for the nucleus. The nuclear magnetic moment orients itself according to the rules of quantum mechanics in the magnetic field of the electrons. The interaction between the electrons and the nuclear magnetic moment produces a splitting of the energy levels of the atom into a number of hfs states.

The magnetic field produced by an electron at the nucleus aries from its orbital motion and its magnetic moment. The orbital motion of the electron produces an $\underline{H}$ which is anti-parallel to $\underline{\ell}$, the orbital angular momentum of the electron. The spin angular momentum of the electron is either parallel or anti-parallel to $\underline{\ell}$. The resultant total angular momentum, $\underline{j}$, is then always parallel to $\underline{\ell}$. Since the contribution to the field at the nucleus due to the electron's magnetic moment is always smaller than that due to the orbital motion, the resultant $\underline{H}$ is always anti-parallel to $\underline{j}$. The same result holds for s-electrons even though the angular momentum is zero. In a few cases, with more than one electron in the jj-coupling, the field is reversed, but these are special cases and need not be considered here. (See Kopfermann, 1945)

The magnetic moment of the nucleus can be considered to arise from the orbital motion of the protons and the nuclear moment of the nucleons. As in the atomic case, the nuclear magnetic moment ($\underline{\mu}$) is proportional to the total angular momentum $\underline{I}$ of the nucleus thus;

$$\underline{\mu} = g(\underline{I})\underline{I} \quad (1.1)$$

where $g(\underline{I})$ is the gyromagnetic ratio of the nucleus in nuclear magnetons.

The spin, I, of the nucleus is the maximum possible projection of $\underline{I}$ in a fixed direction. As in the atomic case,

$$\mu = \frac{ge\hbar I}{2M_p c} \quad \text{where g is the nuclear g factor.}$$

$$= \frac{ge\hbar\, mI}{2mcM_p}$$

$$= g\frac{\mu_o 1}{1838} I \quad \text{where } \mu_o \text{ is the Bohr magneton}$$

and $\mu = g(I)I$ in nuclear magnetons, where a nuclear magneton is defined by $\mu_M = \mu_o\left(\frac{1}{1838}\right)$

A measurement of hfs permits a determination of both I and μ provided the magnetic fields of the electrons at the nucleus can be calculated. The sign of the nuclear magnetic moment is determined by the relative directions of $\underline{I}$ and $\underline{\mu}$; if they are parallel then μ is positive, if anti-parallel then μ is negative.

II. DISCUSSION OF THE PROBLEM.

In this work the hfs of the ground level ($5s^2S_{\frac{1}{2}}$) of CdII has been measured from a study of the resonance lines at λ 2144 and λ 2265, the transitions being $5s^2S_{\frac{1}{2}} - 5p^2P_{\frac{3}{2},\frac{1}{2}}$.

There are eight isotopes of cadmium with an appreciable natural abundance (Table 1), six with even atomic weights and two with odd. The six even isotopes have no measurable magnetic moments

and thus the magnetic hfs in cadmium is expected to be due to the odd isotopes 113 and 111. The approximate concentrations in naturally occurring cadmium are given in Table 1, (Leland and Nier, 1948).

Table 1; Isotope Abundance in Naturally Occurring Cadmium.

A	106	108	110	111	112	113	114	116
%	1	1	12	13	24	12	29	8

A spectoscopic determination of the value of the average nuclear magnetic moment of the odd isotopes in Cd was first obtained by Jones (1933), who studied the transition $6s^2S_{\frac{1}{2}} - 6p^2P_{\frac{3}{2}}$ in the CdII spectrum. This line occurs at $\lambda 8067$ and is especially favorable for interferometric work. However, in the determination of μ, the important Fermi-Segre factor (Fermi-Segre, 1933) was neglected and no correction was made for the unresolved ^2P structure. As well the experimental error was about 10%.

Proctor and Yu (1950) determined the nuclear magnetic moment of Cd by the very accurate nuclear induction method. In this method, the Cd sample is placed in a very strong uniform magnetic field and is subjected to a slowly changing radio frequency field. In this way, transitions are induced between energy levels arising from different orientations of the nucleus in the magnetic field. A measurement of the resonant frequencies provides an accurate determination of the nuclear magnetic moment.

The purpose of this experiment is to measure the hitherto undetermined structure of the 5s level in CdII, to provide a check of the important Fermi-Segre factor, $1 - \frac{d\sigma}{dn}$. In this expression, n is the principal quantum number, and σ the quantum defect so that

$\sigma = n - n_o$ where $n_o = Z_o\sqrt{\frac{R}{T}}$ (2.1) $Z_o = Z$ outer and = 1 for alkali
= 2 for singly ionized alkali earth.

R is Rydberg's constant

T is the term value.

The Fermi-Segre factor occurs in the formula for calculating the nuclear magnetic moment from hfs data. It arises from a relativistic treatment of the many-electron atom. The accuracy of the value of the Fermi-Segre factor as calculated by the method of Crawford and Schawlow (1949) can be tested by a comparison of our results with those of Jones and more significantly by a comparison of Jones and our results with those of Proctor and Yu.

The problem is difficult experimentally due to the high abundance of the even isotopes. The intense components due to the even isotopes, exhibiting no magnetic hfs, tends to obscure the relatively weak components comprising the hfs of the odd isotopes.

Further, the lines for the 5s level are in the far ultraviolet where experimental techniques are difficult. The optical flats used in the Fabry-Perot interferometer must be coated with aluminium films, the optical system must be composed entirely of quartz, and the photographic plates used to record the spectra are of poor sensitivity in this region.

III. THEORY.

Goudsmit-Fermi-Segré Formula.

Goudsmit (1933) obtained an expression giving the hfs in terms of $g(\underline{I})$. This formula was fairly accurate for light elements but failed quite badly when applied to heavier elements. For an s-electron where $j = \frac{1}{2}$, Goudsmit's formula was;

$$g(\underline{I}) = \frac{3an_o^3}{8R\alpha^2 Z_L Z_o^2}\frac{1836}{} \qquad (3.1)$$

Fermi and Segre (1933) proposed a correction to Goudsmit's formula. They started from the empirical formula for the wave function.

$$\psi^2(0) = \frac{1}{\pi a^3 (1-\alpha^2 Z_o^2)^2}\frac{Zi}{2Rh}\frac{dE}{dn} \qquad (3.2)$$

and first dropped the term involving $\alpha^2 Z_o^2$ since for light elements $\alpha^2 Z_o^2 \ll 1$. They first differentiated the Rydberg formula for the

energy

$$E = -\frac{RhZ_o^2}{(n-\sigma)^2} \qquad (3.3)$$

and substituted for $\frac{dE}{dn}$ in 3.2, obtaining

$$\chi^2_{eff}(0) = \frac{Z_i Z_o^2}{\pi a^3 n_c^3}\left(1-\frac{d\sigma}{dn}\right) \qquad (3.4)$$ where $n_c = n-\sigma$

Here they recognize the relativistic correction necessary due to the change in σ with n in ^2S terms.

The formula for g(I) obtained using this expression for the wave function was still not satisfactory and particularly for heavy elements. Breit (1930) and Racah (1931) had shown that relativity corrections are not the same for both components of a fine structure doublet and hence each must be calculated and the difference accounted for in observations. The corrections proposed by them account for this difference and in so doing eliminate the discrepancy which had arisen in earlier calculations involving heavier elements.

The final formulae are;

for s-electrons $$a_s = \frac{8R\alpha^2 Z_i Z_o^2 g(I)}{3n_c^3\ 1838}\, k(\tfrac{1}{2}, Z_i)\ \left(1-\frac{d\sigma}{dn}\right) \qquad (3.5)$$

for non s-electrons $$a = \frac{\Delta\nu\, l(l+1) g(I) k(j,Z)}{Z_i(l+\frac{1}{2})j(j+1)\ 1838\ \lambda(l, Z_i)} \qquad (3.6)$$

Where; R is the Rydberg constant
=109,677.58 cm.$^{-1}$

α is the Sommerfeld's fine structure constant 7.29 x10^{-3}

Z_i is the effective nuclear charge seen by an electron within the closed shells of the atom; = 48 for an s-electron in Cd

Z_o is the effective nuclear charge seen by an electron outside the closed shells of the atom; = 2 for CdII

g(I) is the nuclear gyromagnetic ratio.

σ is the screening constant or quantum defect (See 2.1)

n is the principal quantum number

n_e is the effective principal quantum number (see 2.1)

$$k(j,Z_i) = \frac{4j(j+1)\,(j+\frac{1}{2})}{(4\rho^2-1)} \qquad \text{where } \rho^2 = (j+\tfrac{1}{2})^2 - Z_i^2\alpha^2$$

$$\lambda(\ell,Z_i) = 2\ell(\ell+1)\,\sqrt{\frac{(\ell+1)^2 - \alpha^2 Z_i^2}{\alpha^2 Z_i^2}}\;\; -1-\sqrt{\ell - Z_i^2\alpha^2}$$

$\Delta\nu$ is the fine structure separation.

The Fermi-Segre factor for the 5s electron in CdII was calculated by the method of Crawford and Schawlow (1949). The values of $\frac{d\sigma}{dT}$, n_e, and T are required for this calculation. These values are listed in Table 2. The values of T are taken from Bacher and Goudsmit (1932), n_e is calculated from 2.1, σ is calculated from the definition $\sigma = n - n_e$ and $\frac{d\sigma}{dT}$ is calculated as shown below.

Table 2. t, n, and σ_v for the s-levels in CdII.

ns	T	n_e	σ
5s	136376.6	1.7936	3.2059
6s	53386.4	2.8679	3.1321
7s	29077.1	3.8855	3.1145
8s	18335.5	4.8912	3.1088
9s	12624.3	5.8969	3.1031
10s	9223.2	6.8990	3.1010

From Crawford and Schawlow (1949)

$$\frac{d\sigma}{dn} = \frac{\beta}{\beta - \frac{n_e}{2T}} \qquad \text{where} \qquad \frac{d\sigma}{dT} = \beta$$

For the 5s electron in CdII

$$\beta = \frac{0.0738}{82990.2} = 8.892 \times 10^{-7}$$

$$\frac{n_e}{2T} = \frac{1.7941}{272753.2} = 6.579 \times 10^{-6}$$

$$\frac{d\sigma}{dn} = -0.156$$

and therefore $\quad 1-\frac{d\sigma}{dn} = 1.16$

Substituting the values for the constants and n and $1-\frac{d\sigma}{dn}$ as calculated above, into 3.5, we obtain;

$$g(\underline{I}) = 2.389 \quad a(5s)$$

$$\text{or} \quad a(5s) = 0.4186 \; g(\underline{I}) \qquad (3.7)$$

In a similar manner, using 3.6,

$$a(5p_{3/2}) = 0.0102 \; g(\underline{I}) \qquad (3.8)$$

$$\text{and} \quad a(5p_{\frac{1}{2}}) = 0.062 \; g(\underline{I}) \qquad (3.9)$$

As can be seen from 3.7, 3.8, 3.9, the hfs in the ^{2}P-levels is much smaller than in the s-level and in fact in this experiment was unresolved. However, since one measures from the center of gravity of an unresolved structure and since the distance required is from only one of the components, it is necessary to calculate the distance from the center of gravity of the line to the proper component. (See Calculations). In this way the hfs of only the $^2S_{\frac{1}{2}}$ level is measured (See Figures 1 and 2, also Jackson, 1934).

The total angular momentum of the atom, F can take any one of the values $J+I$, $J+I-1$, $J+I-2$, ---------- $J-I$, where I is the angular momentum of the nucleus and J is the total angular momentum of the electrons.

When $J = 3/2$ and $I = \frac{1}{2}$, then the values that F can have are 2 or 1.

When $J = \frac{1}{2}$ and $I = \frac{1}{2}$, then F can be 1 or 0.

The allowed transitions from $^2P_{1/2}$ are those for which $\Delta F = 0, \pm 1$ with $0 \not\to 0$ forbidden and are therefore represented by the lines a, b, and c in Figures 1 and 2.

IV. SOURCE.

Every spectral line has a width which is due to the physical properties of the source. The sources used in studying atomic spectra have a line width sufficient to obscure most hyperfine structure. Special sources have been designed to overcome this difficulty. A brief survey of the major causes of line broadening follows. A more detailed discussion can be found in Tolansky (1947).

Natural line width arises from the uncertainty of the energy of any spectral line. The lifetime of an excited state is of the order of 10^{-8} sec. Heisenberg's Uncertainty Principle shows that $dEdt \sim h$. The quantity dE is a measure of the uncertainty in the energy and thus the frequency spread in any spectral line. The natural line width is usually small and may be neglected. At 2000 A it is approximately 0.003 cms^{-1}. This is small compared to other sources of line broadening.

Pressure broadening is caused by the perturbations of the energy levels of an atom due to collisions between atoms. When the pressure of the gas in which the emitting atoms are situated is high, the collision frequency is also high and the pressure broadening may be large. However, pressure broadening is negligible if the pressure is the order of a few millimeters.

Zeeman and Stark broadening arise from electric and magnetic fields respectively. When emitting atoms are placed in an electric or magnetic field, the energy levels are split. The magnitude of the splitting depends on the field strength. Care must therefore be taken that the applied fields are not too large, although the problem is not serious for non-hydrogenic atoms.

Doppler broadening is the most important cause of line width. It is due to the random thermal motion of the atoms and the consequent Doppler shift of the radiation. Owing to a Maxwellian distribution of velocities in a gas, the final line shape is Maxwellian and the half-width is

$$\Delta\nu = 2\sqrt{\log 2}\,\sqrt{2RT/Mc^2}\,\nu \text{ cms.}^{-1}$$
$$= 0.71 \times 10^{-6}\sqrt{T/M}\,\nu \text{ cms.}^{-1}$$

Where ν is the frequency in wave numbers
T is the absolute temperature
M is the molecular weight.

In the study of a specific element, the molecular weight is fixed, but the Doppler width can be decreased by using a transition with a low ν. The width can be further decreased by lowering the temperature of the source. This can be accomplished in several ways. Cooling agents are usually used and the most common ones are water, acetone and dry ice, and liquid nitrogen. Liquid hydrogen and liquid helium have been used but they involve a complicated technique, and the input energy to the sources must be very low due to the low latent heats of these liquids.

An atomic beam is an important alternate method of obtaining a source with a low effective temperature. Atoms of the element under study are evaporated in a chamber where the pressure is such that the mean free path of the atoms is greater than the dimensions of the chamber. The stream of atoms is collimated by slits to form a narrow beam. The beam is excited by electron bombardment and the resultant emission spectrum is viewed at right angles to the beam, therefore at right angles to the direction of motion of the atoms. In this way the Doppler broadening is considerably reduced.

The source used in this experiment was a modified Schuler hollow cathode discharge tube, shown in Figure 4. The cathode is an aluminium cone mounted in a copper block. This in turn was joined to the rest of the discharge tube by a copper-to-glass seal. The hole in the aluminium cone was 0.45 cm. in diameter and 0.9 cm. deep. The source was cooled by liquid nitrogen in a Dewer flask which completely enclosed the source to a height denoted by H on Figure 4. The aluminium cone was lapped to fit into the copper block so as to ensure good thermal contact between the copper and aluminium. The amount of heat conducted down the glass to the cathode is negligible and thus the temperature of the carrier gas would be very close to the coolant. This reduces the

Doppler width. The field broadening of the lines in this type of source is small. The anode was an aluminium cylinder connected to the exterior by tungsten wire passing through the glass tubing and sealed in by a tungsten-to-glass seal.

A few pieces of pure cadmium were placed in the hole in the aluminium cone. These had to be periodically replaced during the experiment since they became coated with a sputtered aluminium film resulting in a decrease in the intensity of the cadmium spectrum lines.

Neon was chosen for the carrier gas due to its suitable sputtering of Cd, and due to the lack of neon lines in the 2144-2265 region. Pure neon was stored in a 1-litre flask separated from the system by two stopcocks in series (Figure 3). A small amount of neon could thus be released into the system. The amount of neon in the source could thus be controlled and the pressure of the gas kept at a suitable value. The pressure in the source was measured by the Crooke's dark space around the electrodes in a sidearm discharge tube excited by an induction coil. The most satisfactory pressure for the discharge obtained with a Crooke's dark space of about 1.5 mm. corresponding to a pressure of 4 mm. Hg. (J. J. Thomson, 1928). The neon was not circulated in this experiment since satisfactory cleaning of the neon was obtained by the use of a sidearm containing charcoal cooled by liquid nitrogen. This served to absorb any gaseous impurities that were released into the system.

Each day the neon of the previous day's run was pumped out. At the same time, the charcoal trap was cleaned by heating it with a bunsen burner, driving off any of the impurities that had been absorbed the previous day. When there was no trace of a discharge in the system when tested by a high frequency coil, the pumps were cut off and the system refilled with neon.

The pumping system consisted of a mercury diffusion pump backed by a rotary pump. The discharge tube could be isolated from the pumps

by the vacuum valve V in Figure 3. Between this valve and the mercury diffusion pump was a mercury vapor trap, consisting of a U-shaped bend in the glass tubing around which could be placed a dewar filled with acetone and dry ice. This was cold enough to condense any mercury vapor that might otherwise diffuse back to the discharge tube. In addition a large jar served as a vacuum resevoir, giving stability to the vacuum system which except for this had a very small volume.

V. OPTICAL SYSTEM.

The light from the discharge passed from the source through a quartz window sealed onto the discharge tube by Apiezon wax (Figure 4) It then passed through a quartz lens and was reflected at right angles by a front-surfaced aluminium mirror through a second lens (Figure 5)

The following procedure was used to line up all the components of the optical system on the same axis. The lenses and interferometer were removed, having only the mirror to reflect the light from the source into the spectrograph. The source was then placed on the axis of the spectrograph, defining the axis of the system. The first two lenses were then replaced. These had to be adjusted so that parallel light fell on the interferometer. Since the spectral lines studied here were in the ultra violet and since the focal length of a lens changes with wavelength, it was impossible to make this adjustment using visible light. Rather, the positions of the lenses were determined approximately by calculating the focal lengths from formulae at these wave lengths. The lenses were accurately positioned by using a fluorescent screen at the plate holder of the spectrograph and observing the position of best intensity as the lenses were moved about their approximate positions. The interferometer was then placed on the axis of the system. It was mounted externally to the spectrograph and its support was bolted to the spectrograph to minimize the trouble caused by vibrations. The light emerging from the interferometer was focussed by a third lens on the slit

of a Hilger Medium Quartz Spectrograph. (f/10). To make a sharp focus of the fringes this lens was moved one mm. at a time and a photograph of the fringes taken at each position. The sharpest photograph determined the placement of the lens. Fringes which are a long way from the centre of the pattern were used during this focus.

The interferometer and the spectrograph were housed in a separate room. In this way the changes of temperature at the interferometer were minimized.

A number of Eastman and Ilford photographic plates were tested for the recording of the spectra. The Ilford Q_1 and Q_2 plates were found to be the most satisfactory and were used throughout the remainder of the experiment.

VI. EXPERIMENTAL OBSERVATIONS.

Three different currents were used in the discharge, 5, 10, and 15 ma. The currents were purposely kept low, since the heat produced in the discharge is proportional to I^2, and the greater the heat production, the greater the Doppler broadening of the lines. However, since there was little apparent difference between the results obtained with 5 and 10 ma. currents, and since the 5 ma. exposures took longer thus introducing difficulties due to the changing atmospheric conditions, temperature and pressure, most results were obtained with 10 and 15 ma. currents. With these currents, exposures were of the order of 15 minutes.

Two interferometer spacers were used, 0.518cm. and 1.255 cm. The fringe patterns showed three components. The central and very intense component was ascribed to the even isotopes, and the other two ascribed to the odd isotopes. The distance between these two side components, with a small correction, gives the splitting of the $5s^2S_{\frac{1}{2}}$ level. Designating the strong central component by $\dot{0}$, the weaker of the side components by w, and the strong side component by s , the

following results were obtained from measurements with a travelling microscope.

Table 3. Hfs in λ2144 of CdII

Spacer	Method of Measurement	Number of Orders	Current	$\Delta\nu(0,w)$ cms^{-1}
0.518	off-center	14	15ma.	.337 cm^{-1}
0.518cm	"	16	15	.332
0.518	"	5	15	.328
0.518	on-center	6	15	.312
0.518	off-center	15	15	.337
0.518	on-center	2	15	.320
0.518	off-center	3	15	.320
0.518	"	15	15	.328
0.518	"	10	15	.325
0.518	on-center	2	15	.320
0.518	"	2	15	.332
0.518	"	3	15	.335

Average; $\Delta\nu(0,w) = 0.329 \pm 0.008$ cm^{-1}

Table 4, Hfs in λ2144 of CdII

Spacer	Method of Measurement	Number of Orders	Current	$\Delta\nu(s,w)$ cms^{-1}
1.255 cm	on-center	1	15ma.	0.518 cm^{-1}
1.255	on-center	5	15ma.	0.520
1.255	on-center	7	15	0.522
1.255	on center	5	15	0.526
1.255	on-center	1	15	0.513
1.255	on-center	3	15	0.513
1.255	on-center	3	15	0.524
1.255	on-center	7	15	0.517

Average; 0.519 ± 0.004 cm^{-1} = $\Delta\nu(s,w)$

Table 5. Hfs in λ2265 of CdII

Spacer	Method of Measurement	Number of Orders	Current	$\Delta\nu(0,s)$cm^{-1}
0.518cm	off-center	7	10ma.	0.356 cm^{-1}
0.518	off-center	7	15	0.354
0.518	off-center	7	15	0.357
0.518	off-center	7	10	0.358
0.518	off-center	7	10	0.355
0.518	off-center	14	15	0.374
0.518	off-center	14	15	0.370
0.518	off-center	8	10	0.359
0.518	off-center	6	15	0.366
0.518	off-center	6	15	0.362
0.518	off-center	6	15	0.358
0.518	on-center	7	15	0.367
0.518	on-center	7	15	0.366
0.518	on-center	7	15	0.357

Average; 0.362 ± 0.005cm^{-1} = $\Delta\nu(0,s)$

Table 6. Hfs in λ2265 of CdII

Spacer	Method of Measurement	Number of Orders	Current	$\Delta\tilde{\nu}$(s,w) cm^{-1}
1.255cm	on-center	1	10ma	0.494cm.$^{-1}$
1.255cm	on-center	3	10ma	0.483
1.255	on-center	6	10	0.485
1.255	on-center	6	10	0.497
1.255	on-center	3	10	0.474
1.255	on-center	6	10	0.505
1.255	on-center	2	10	0.489
1.255	on-center	3	10	0.496
1.255	on-center	6	10	0.498

Average; $0.491 \pm 0.007 cm^{-1} = \Delta\tilde{\nu}$ (s,w)

The term "on-center" refers to measurement across the diameter of a fringe. This technique was used whenever possible, ie. when the fringe was in focus on both sides of the center of the fringe system. On some plates, the fringe system would be in sharp focus on only one side of the center, in which case, the "off-center" method of obtaining fringe diameters was used (Tolansky, 1947)

The errors quoted in these tables are the average deviations from the mean of the individual readings.

The separation (s,w) could be measured directly only on the plates obtained with one spacer, 1.255 cm. While it would appear that the (s,0) and (0,w) measurements obtained with the other spacers could have been added to give the structure (s,w), the difficulty of setting the cross hairs of a measuring microscope on the center of the over - exposed central component, 0, would have subjected the results so obtained to a large error.

VII. Calculations.

^2P Correction:

As pointed out in Section III (Theory), the allowed transitions from $^2P_{3/2}$, $_{1/2}$ are those represented by the lines a,b, and c in Figures 1 and 2. However the lines b and c were not resolved in this experiment although the distance required for the calculation is that between a and c for λ 2144 and between a and b for λ 2265.

The distances (s,w) quoted in Tables 3 to 6 are actually measured from center of gravity of this unresolved doublet. It is therefore necessary to calculate the distance from the center of gravity to each of the components using the relative intensities of the components.

For λ2144, the relative intensities of the lines b and c are b:c = 5:1. The center of gravity of the system is therefore $\frac{1}{6}a(5p_{3/2})$ This separation is designated by a'.
to the high frequency side of b. $\Lambda a'(5p_{3/2})$ is the hfs in the $5p_{3/2}$ level.

Similarly for λ2265, the intensity ratio is b:c = 2. Consequently the center of gravity is $\frac{1}{3}a(5p_{\frac{1}{2}})$ to the high frequency side of b, this separation being denoted by a".

To calcualte a' and a" one must first have the values for $a(5p_{3/2})$ and $a(5p_{\frac{1}{2}})$. One first finds an approximate value for g(I) using the uncorrected values for a(5s) from Tables 4 and 6 in(3.7). These values for g(I) are then substituted into (3.8) and (3.9), giving $a(5p_{3/2}) = 0.0124$ cm.$^{-1}$

and $a(5p_{\frac{1}{2}}) = 0.072$ cm.$^{-1}$ Therefore

a' = 0.002 cm.$^{-1}$

and a" = 0.024 cm.$^{-1}$

For λ2144 $a(5s) = \Delta\nu(s,W) + a(5p_{3/2}) - a'$

$= 0.519 + 0.0124 - 0.002$

$= 0.529$ cm.$^{-1}$

For λ2265 $a(5s) = \Delta\nu(s,W) - a''$

$= 0.467$ cm.$^{-1}$

Substituting these value for a(5s) into equation 3.7, one obtains for λ2144, g(I) = -1.26, and for λ2265, g(I) = -1.12. The average g(I) is -1.19. From equation 1.2 and using $I = \frac{1}{2}$ (Poss, 1949) $\mu = -0.59$ nuclear magnetons. ($I = \frac{1}{2}$ for both Cd^{111} and Cd^{113})

This value of μ must be increased by 2% to account for the

finite size of the nucleus (Rosenthal and Breit, 1932). This gives a final value of $\mu = -0.60$ n.m.

Isotope Shift.

An attempt was made to calculate the isotope shift between the even and odd isotopes from the displacement of the broad central component. In the $^2S_{\frac{1}{2}}$ level, the distances of the two components from the zero positions should be in inverse proportion to their values of $2F+1$ i.e. 3:1. (See accompanying figure). The zero position should be represented by the central line. If the values for (s,0) and (0,W) are compared and found not to be in the ratio of 3:1, then the discrepancy can be attributed to the displacement of the central line due to isotope shift.

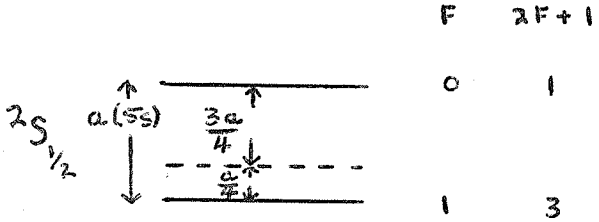

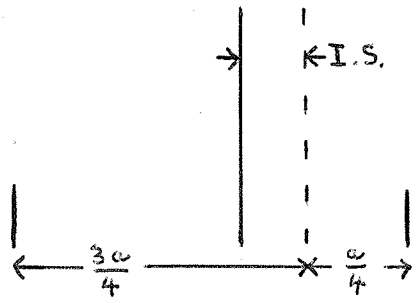

The data for λ 2144 gave an isotope shift between the average position of the even and odd isotopes of 0.061 cm^{-1}. The data for λ 2265 gave an i.s. of -0.047 cm^{-1}. The inconsistency of the results is attributed to the difficulty of accurately locating the center of the broad component. No conclusions could be drawn about the isotope shift.

VIII. Discussion of the Results.

The value of μ obtained here is subject to an error of about 6%. Thus the average value of the nuclear magnetic moments of the two odd isotopes of cadmium is $\mu = 0.60 \pm .03$ n.m.

The value of the Fermi-Segre factor for the 6s electron in CdII is 1.03. Applying this and the correction for the unresolved ^2P structure to Jones' results for the 6s $^2S_{\frac{1}{2}}$ level the value of μ is $\mu = -0.63$n.m. The values of μ from these two spectroscopic determination agree within experimental error, indicating the usefulness of the Fermi-Segre factor.

A more significant confirmation is provided by a comparison of these results with those of Proctor and Yu (1950). The result from their accurate nuclear induction method is $\mu = -0.608$ n.m. Our figure is in close agreement with their value, confirming the Fermi-Segre factor when calculated by the method of Crawford and Schawlow.

APPENDIX 1.

Fabry-Perot Interferometer.

The high resolution required in this experiment was obtained with a Fabry-Perot interferometer. This instrument consists of two optical flats separated by a fixed spacer so that they are parallel to one another.

When the interferometer is used to resolve lines with λ's longer than 4000A, the optical flats are usually coated with silver films. However, in the region below 4000A, the reflection coefficient of silver films falls off and the fringes produced are not sufficiently sharp. Aluminium films are generally used for studying lines in the ultraviolet. While the properties of Aluminium films in the ultraviolet are not as good as those of silver films in the red region of the spectrum, the reflection coefficients of properly prepared films are sufficiently high to give a large resolving power.

The optical flats used in the ultraviolet must be made of quartz. One pair of crystalline quartz plates of very high quality made by Adam Hilger and Co. was available for these experiments.

The basic equation of the Fabry-Perot interferometer is:

$$n\lambda = 2t\mu\cos\theta \qquad \text{A.1}$$

Where t is the separation of the plates,

n is the order of interference of the fringe,

λ is the wavelength of the incident light,

μ is the refractive index of the medium between the optical flats

θ is the semi-angle of the cone along whose surface the incident light travels.

For small θ, at or near the center of the fringe system, $\cos\theta = 1$. Substituting the wave number $\bar{\nu}$ for $\frac{1}{\lambda}$ and differentiating one obtains:

$$d\bar{\nu} = \frac{dn}{2\mu t} \qquad (A.2)$$

On moving from one fringe to the adjacent fringe of the same system, dn changes by one. In practice the interferometer is used in air where $\mu = 1.00$. Thus, the interorder separation is $\frac{1}{2t}$ cm.$^{-1}$

A very small energy difference between two lines of a spectrum can be measured by the correct use of the correct spacer. If the resolving limit of an interferometer is $\frac{1}{15}$ of an order, then one must use a spacer such that the difference in energies of the two lines is greater than $\frac{1}{15} \frac{(1)}{2t}$, where t, the distance between the plates of the interferometer, is the width of the spacer.

The shape of the fringe, and thus the resolving power of the instrument, is essentially proportional to $\frac{1}{1-R}$, where R is the ratio of reflected to incident light. Also

$$\frac{I}{I_0} = \frac{1}{(1+\frac{A}{T})^2} = \frac{T^2}{(1-R)^2} \qquad (A.3)$$

where T is the transmission coefficient

A is absorption coefficient

R is the reflection coefficient.

and $R + A + T = 1$.

Thus for best results, films with as large as possible R must be produced under conditions which keep the ratio $\frac{A}{T}$ at a minimum. In practice a compromise must be made between high resolving power and a high intensity.

The most satisfactory method of coating interferometer plates with metal films is by the method of vacuum evaporation. Burridge et al (1953), have studied the preparation of aluminium films and have measured the reflection and transmission coefficients in the ultra-violet region. They have shown that films of optimum quality are produced provided that $pt = 3$, where p is the pressure in mm. $\times 10^{-5}$ of Hg, and t is the time

of evaporation in minutes. Under these conditions values of $R + T = 90\%$ can be obtained. With these plates, a resolving power of $\frac{1}{18}$ of an order was obtained without excessive loss of intensity.

The values of pt recommended by Burridge are smaller than those that have been used in the past. The higher quality of the films so produced is explained by Burridge on the basis of fewer chemical impurities in their films. The lower the value of pt, the lower is the probability of an impurity atom striking the plates during evaporation and becoming incorporated into the films. However in order to evaporate in a shorter time, a higher current must be used, thus increasing the probability of releasing absorbed gases from the vacuum chamber. A proper balance must be obtained between excessive heating and time of evaporation.

The plates used in this experiment were produced at a value of $pt = 4$ (See Evaporator - Appendix 2). With these films $\frac{1}{8}$ order could be resolved. This was sufficient for the measurements made in this experiment.

Only a limited change in atmospheric pressure can be tolerated during any one exposure due to the displacement of the fringes caused by change of refractive index. The change that could be tolerated was calculated to be 0.05 cm. Hg. At such times as the pressure was expected to change quickly, the exposures were abandoned. The refractive index of air is also affected by a change in temperature (Δt). Since the room was closed, Δt was usually small and presented no difficulties.

Appendix 2.

The Evaporator.

The evaporator constructed for these experiments was based on the design of Ritschl, 1931. In this design, the evaporating filament is placed at the center of a vacuum chamber. The interferometer plates are placed one at the end of each of two horizontal side arms so that both plates can be coated simultaneously with approximately equal metallic films. A schematic diagram is shown in Figure 6.

The center box (A-Figure6) of the evaporator, is a 9" cube made of bronze castings. The horizontal side arms (B-Figure 6) are made of 6" brass tubing and are hard-soldered to the center box. Their lengths were chosen so that the thickness of the metallic films deposited on the interferometer plates would differ by less than 1% over the area of the plate, if the metal were considered to have been evaporated from a point source on the axis of the plates. Since the construction of the filament is such that the source of the aluminium vapor is an extended one the difference is considerably less than 1% (Figure 9)

The interferometer plates were clamped onto holders (Figure 7). These were held in position during evaporation by three clamps soldered on the inside and near the ends of the side arms (C-Figure 6). The open design of the plate holders permitted a free flow of air from behind the holders during evacuation of the system. At the pressures required for evaporation, the mean free path of the molecules is of the order of 5 meters. Thus any molecules separated from the system by a barrier with a small aperture would diffuse into the system over a long period of time, constituting a slow air leak. This would prolong the evacuation time.

The ends of the side arms were closed by brass plates (D-Figure 6) which were bolted into place. The vacuum seal was provided by an o-ring which was compressed into a machined groove in accordance to the manufacturer's specifications. Glass windows were fitted into the end

plates and sealed with Apiezon W. In this way one could observe the progress of the evaporation.

A brass tube of the same diameter as the side arms but considerably shorter (E-Figure 6) was attached to the top of the center box. This was also sealed at the end by a brass plate compressing an o-ring into a machined groove. Through this plate passed two brass tubes which conducted the current to the filament (N-Figure 6). The tubes had to be electrically insulated from each other and from the box and as well there must be a vacuum seal around the tubes. This was accomplished by the design shown in Figure 8. The bakelite pieces A and B provided the insulation while two o-rings were compressed into the grooves C and D. The brass tubes were water-cooled to prevent the melting of the solder joints due to the heat generated by the heavy current required to melt and evaporate the aluminium on the filament.

The filament was bolted onto the bottom of these conductors in such a position that it was centered on the axis of the plates and parallel to them. The filament was made of 0.040 in. tungsten wire. The shape of the filament is shown in Figure 9. Pieces of aluminium foil were wound around each of the eight valleys in the filament. In this way an extended source of aluminium was obtained.

A pair of vanes connected to a piece of soft iron was set in the center box. The vanes were large enough so that when they were in position, they shielded the interferometer plates from anything evaporated from the filament during outgassing (See Operation of the Evaporator). The vanes could be rotated with an external magnet exposing the plates when the aluminium was to be evaporated.

The tube connected onto the bottom of the box was again 6" in diameter and somewhat longer than the top tube (F-Figure 6). This tube

provided the connection between the pumping system and the evaporation chamber. As well, there was a liquid air trap set in the tube (Figure 10). This is a vacuum-tight chamber set inside the vacuum system into which liquid air could be poured from the outside. This provided a cold surface within the chamber for the condensation of organic vapors. The conduction of heat to this chamber was kept to a minimum by the use of thin walled german silver tubes to support the trap and through which the liquid air was poured into the trap (Figure 10).

Connected onto the bottom of this lower tube was a water-cooled baffle (G-Figure 6). Below this was an oil-diffusion pump (MC 275) with a pumping speed of 275 litres/second (H-Figure 6). A high vacuum valve (I-Figure 6) could be used to isolate the oil-difussion pump from the mechanical fore pump (J-Figure 6), so that the performance of the mechanical pump could be tested. The speed of the diffusion pump was matched to that of the fore pump.

Pressure readings could be taken at two places in the system. A Pirani gauge (K-Figure 6) which was effective down to 10^{-3} mm. Hg was placed between the valve and the mechanical pump. This enabled one to check the backing pressure against which the diffusion pump was working. A ground glass fitting was set into one side arms of the evaporator near the position of the interferometer plates during evaporation. Either a Phillip's cold cathode ion gauge reading down to 10^{-5} mm. Hg or an Edward's ionisation gauge (down to 10^{-8} mm. Hg.) could be used in this fitting. For leak testing and for the actual evaporation, the cold cathode gauge was used while the ionisation gauge was used to determine under what conditions the system was capable of reaching a satisfactory pressure.

The commercial power supply and measuring devices for the ionisation gauge were not available for this experiment. The instruments

used for these purposes were designed from a knowledge of the properties of the ionisation gauge and were constructed from pieces of laboratory equipment. These proved quite satisfactory for measuring static or slowly changing pressures but due to the rapid variations of the emission of the gauge filament during evaporation, adjustments could not be made quickly enough to make an accurate measurement of the pressure during evaporation. Therefore the cold cathode gauge and its commercially available control panel was used to measure these pressures.

Some difficulty was encountered in obtaining the low vacuum necessary for producing good films. Some of the brass plates were made from castings and these proved troublesome due to the presence of blow-holes. All of the units made of castings were then tinned, inside and out, sealing some holes. A few large leaks were then located by creating a positive pressure of about 15 lb./sq. in. inside the apparatus and watching for bubbles when a soap solution was poured over the outside. A number of tests were performed to find the smaller leaks still present in the system. First a brass plate was sealed into the bottom of the central box and the pumps turned on. A low pressure was quickly reached indicating that the part of the system thus sealed off was not at fault. The suspected surfaces were then sprayed with hydrogen, the pressure gauge being watched for any deflection. This test proved inconclusive. The surfaces were then sprayed with acetone, pressure fluctuations again being noted. This also was inconclusive. Various sections of the evaporator were covered with Apiezon Sealing Compound Q with no positive results. Finally, however, the holes were sealed by painting the whole unit with glyptal while the pumps were in operation. Presumably the glyptal was forced into the small holes by atmospheric pressure so that they were sealed.

Operation of the Evaporator.

When coating the interferometer plates used in this experiment, the following procedure was followed. The filament was bent to the shape shown in Figure 9. It was then set in the evaporator with no aluminium on it, and the pressure in the system lowered to 0.05mm. Hg. A heavy current (the same as used in evaporation) was then passed through the filament thus cleaning and outgassing it. The filament was then removed from the apparatus and loaded with 140 mgm. Aluminium foil in the eight valleys of the filament. This amount of aluminium had been determined from the results of previous runs as the amount required to give the proper reflection coefficient. The plates were then washed in concentrated HCl to remove the films deposited previously, washed in a commercial detergent and dried with clean absorbant cotton. After the filament and the plates were in position the system was again evacuated and when the pressure as measured by the cold cathode gauge was 2×10^{-5} mm. Hg., a current was again passed through the filament for a short time to melt and outgas the aluminium. When the pressure was again reduced to 2×10^{-5} mm. the vanes which up to now had been covering the plates were rotated by means of the external magnet, exposing the plates. The aluminium was then evaporated in a period of about 15 seconds during which time the pressure rose to about 15×10^{-5} mm. The value of pt for the evaporation was then about 4 which was somewhat larger than the value suggested by Burridge.

The transmission coefficients for these films were then measured using white light, a blue filter and a commercial light meter. From the curves of Burridge et al the transmission coefficients at 2200 A could then be determined. These were the same for the two plates and equal to 2.2%. This corresponds to a value of 90% for R+T and thus A = 10%. From A.3, this gave the intensity of the fringe maxima to be $\frac{1}{20}$ that

of the incident light. Although this is a severe reduction in intensity, there was still sufficient light to give satisfactory exposures without unduly long exposure times.

In conclusion, the author would like to thank the National Research Council of Canada for their substantial financial assistance which enabled this work to be done.

The author would also like to thank Dr. F. M. Kelly, Associate Professor, Department of Physics for his advice and direction throughout the course of the experiment.

REFERENCES

Bacher, R. F. and Goudsmit, S 1932. Atomic Energy States. McGraw Hill Book Co., New York.

Breit, G. 1931. Phys. Rev. 38,463.

Burridge, J. C., Kuhn, H. and Pery, A. 1953. Proc. Phys. Soc. B.66,963.

Crawford, M. F. and Schawlow, A. L. 1949. Phys. Rev. 76,1310.

Fermi, E. and Segre, E. 1933. Zeits. F. Phys. 82,729

Goudsmit, S. 1933. Phys. Rev. 43,636

Jackson, D. A., 1934. Proc. Royal Soc. A, 147,500

Jones, E. G. 1933. Proc. Phys. Soc. 45,625.

Kopfermann, H. 1945. Nuclear Magnetic Moments, J. W. Edwards, Ann Arbor, Michigan, U. S. A.

Leland, W. T. and Nier, A. O. 1948, Phys. Rev. 73,1206

Proctor, W. G. and Yu, F. C. 1950, Phys. Rev. 76,1728

Poss, H. L. 1949. Properties of Atomic Nuclei, I. Spins, Magnetic Moments and electric Quadrapole Moments. Brookhaven National Laboratory, Upton, New York, U.S. A.

Racah, G. 1931. Zeits. f. Phys. [illegible]. 71, 431

Ritschl, R. 1931, Zeits. f. Phys. 69,578.

Thomson, J. J. 1928, Conduction of Elecricity Through Gases, University Press Cambridge, England.

Tolansky, S. 1947. High Resolution Spectroscopy, Pitman, New York, U.S.A.

Vinti, J. P. 1939. Phys. Rev. 56,1120.

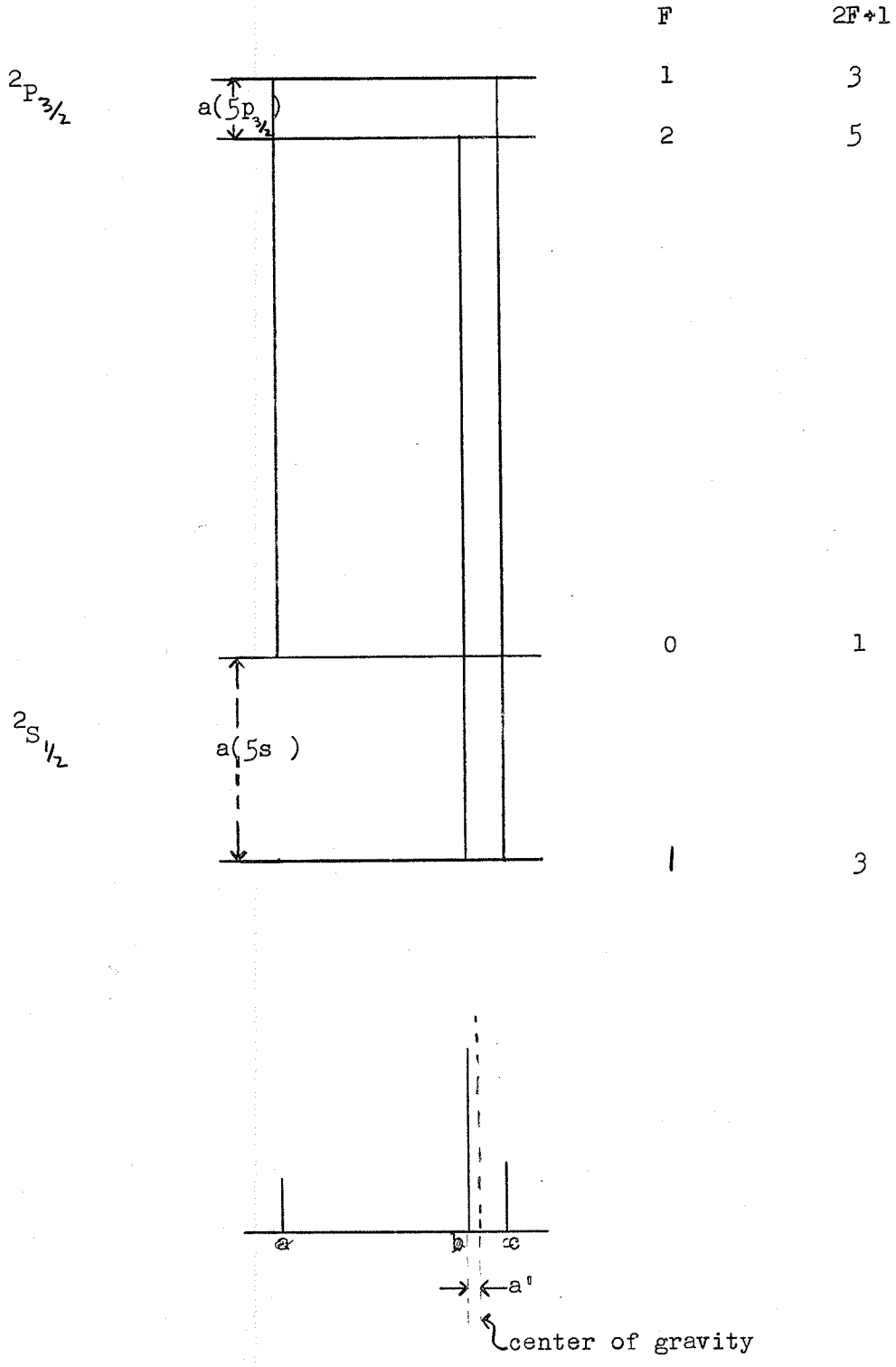

Figure 1. The Hyperfine Structure in the terms $^2S_{1/2}$ and $^2P_{3/2}$ and the allowed energy changes (Not to scale)

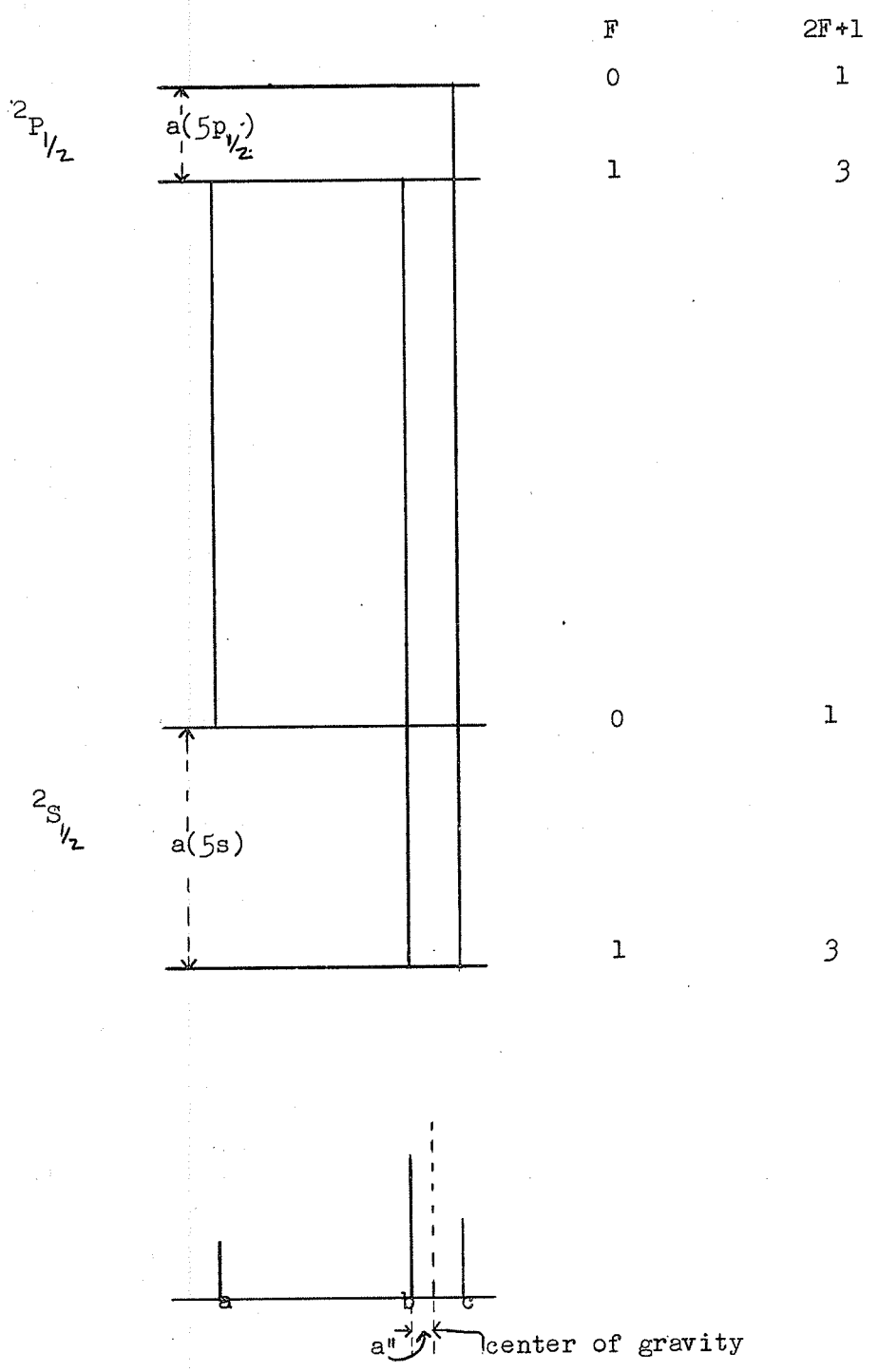

Figure 2. The Hyperfine Structure in the terms $^2S_{1/2}$ and $^2P_{1/2}$ and the allowed Energy Changes. (Not to scale)

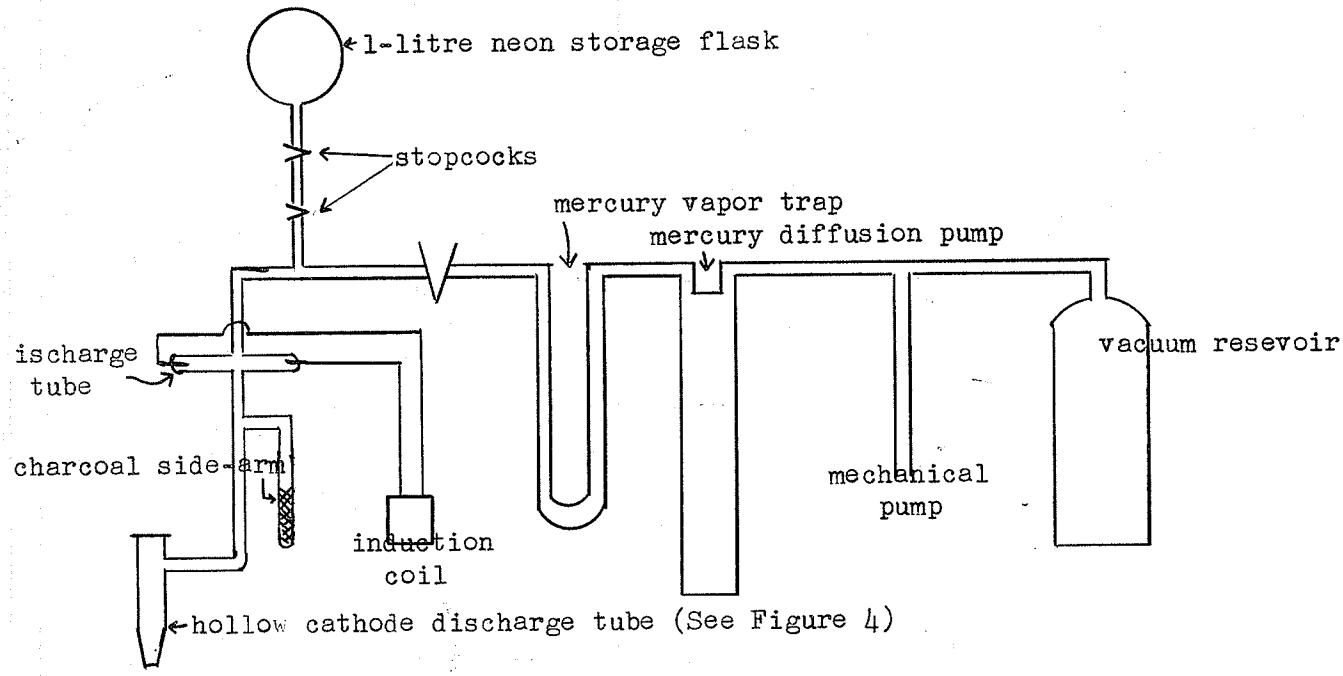

Figure 3. Source

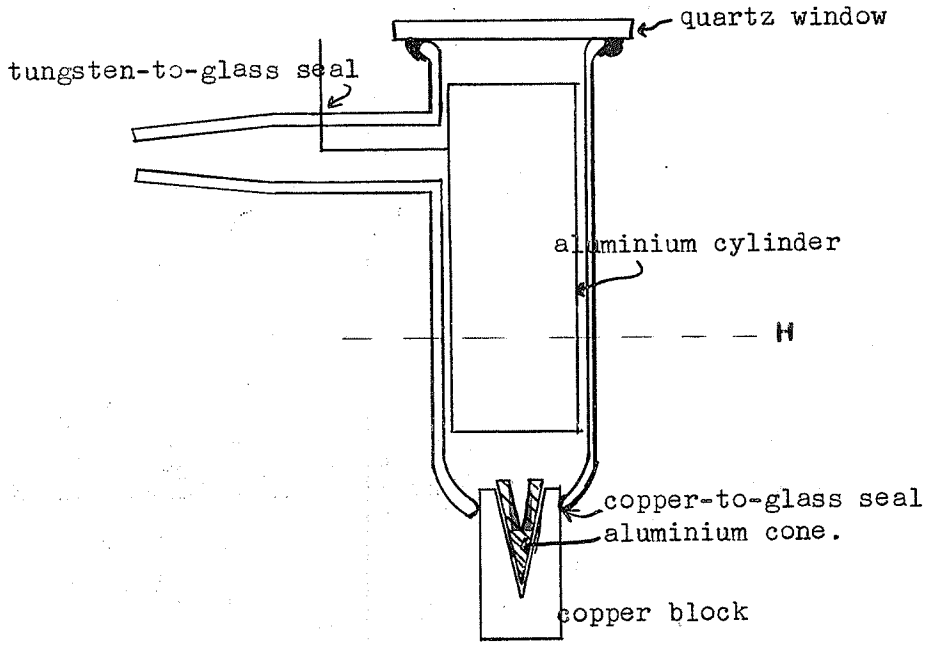

Figure 4. Hollow cathode Discharge tube.

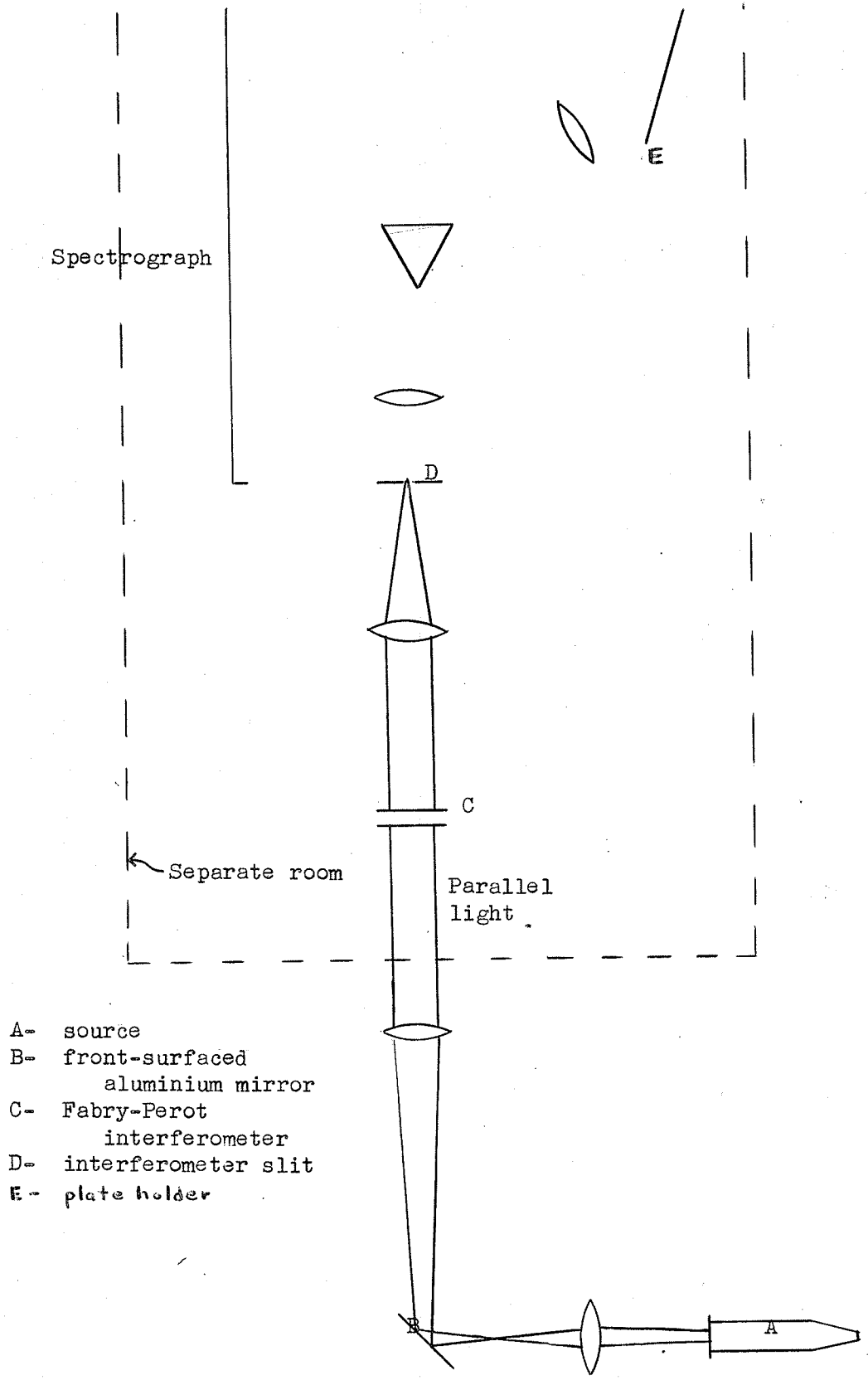

Figure 5. Optical System.

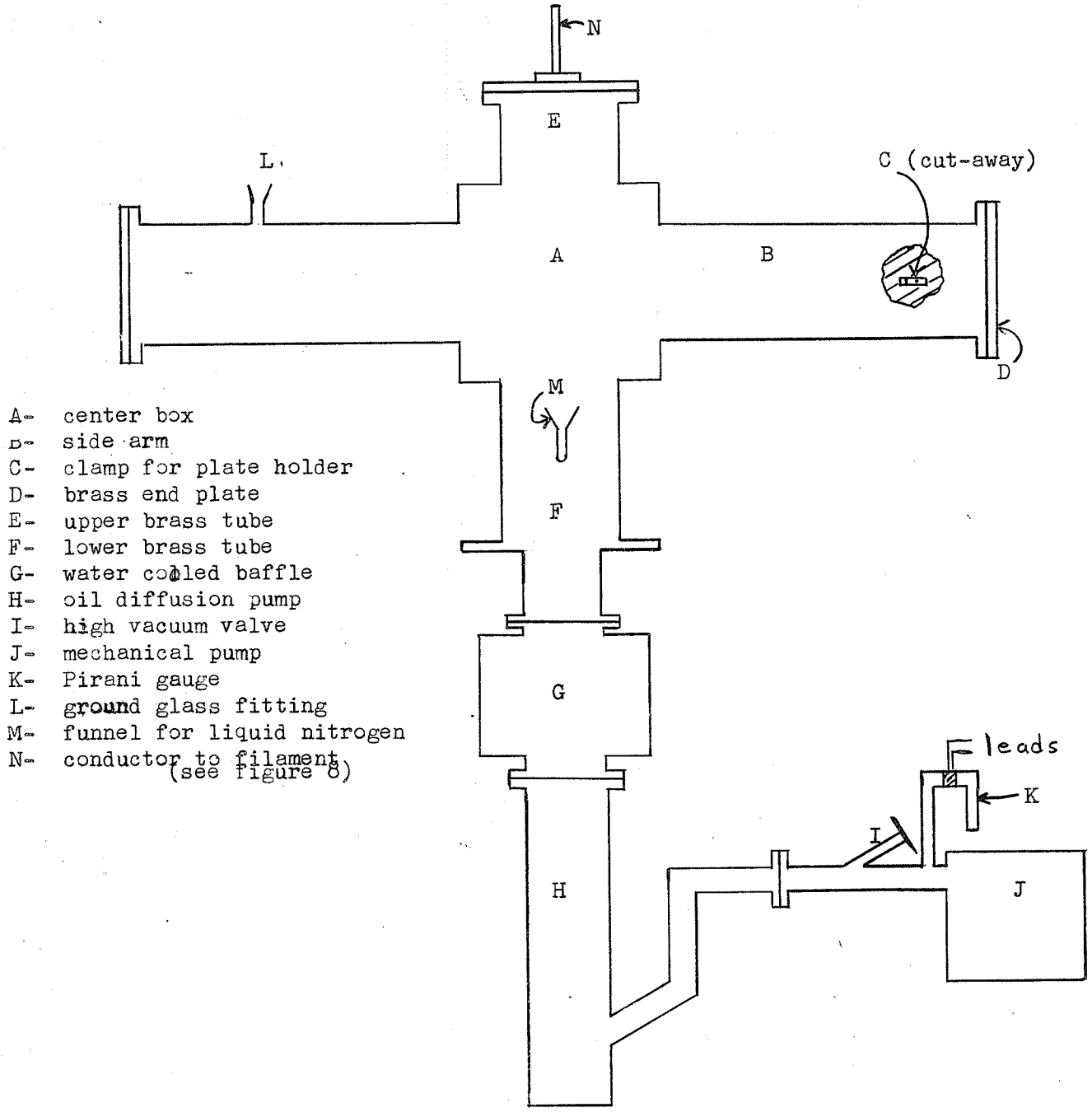

A- center box
B- side arm
C- clamp for plate holder
D- brass end plate
E- upper brass tube
F- lower brass tube
G- water cooled baffle
H- oil diffusion pump
I- high vacuum valve
J- mechanical pump
K- Pirani gauge
L- ground glass fitting
M- funnel for liquid nitrogen
N- conductor to filament (see figure 8)

Figure 6. Front view of the Evaporator and Pumping System.

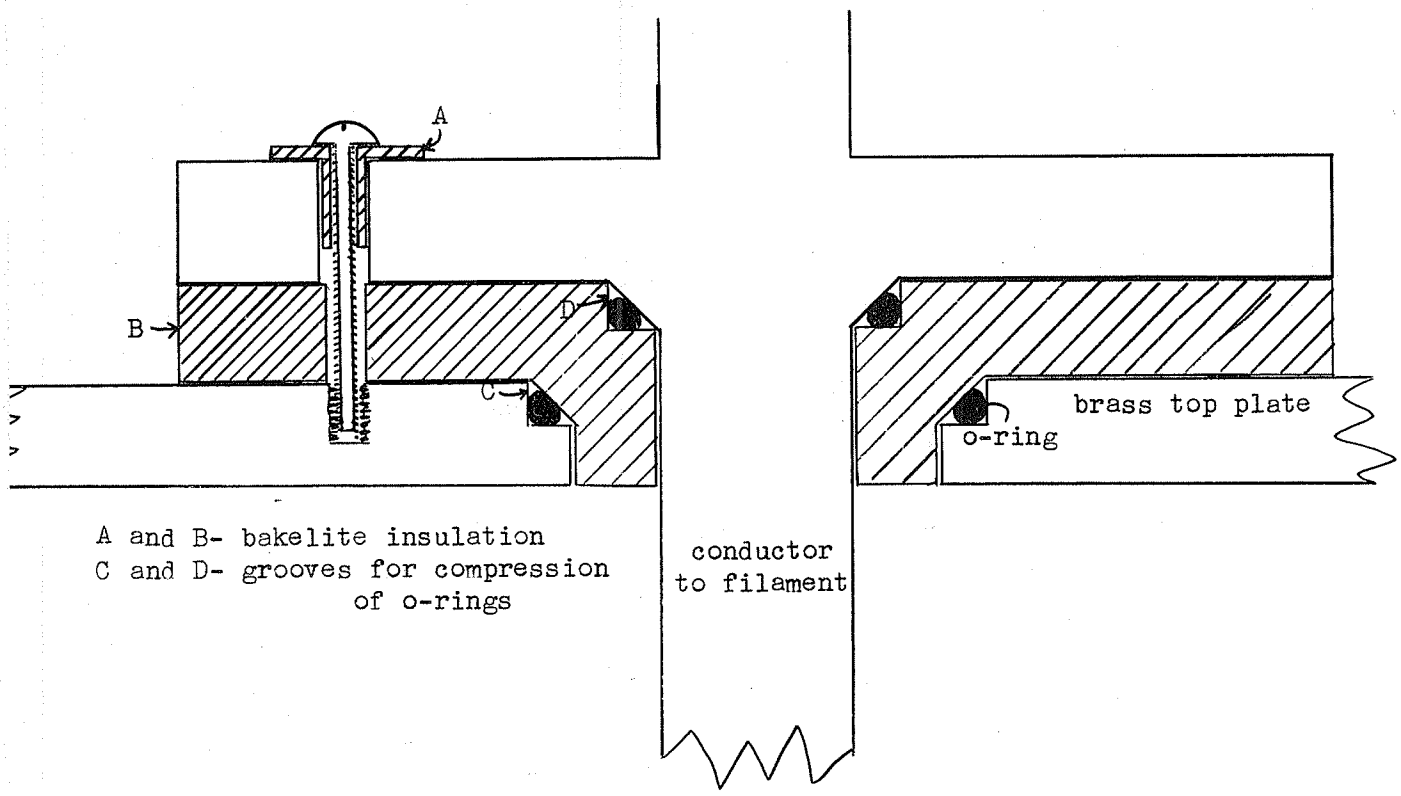

Figure 8. Design of Vacuum seal and Electrical Insulation for Conductors to Filament.

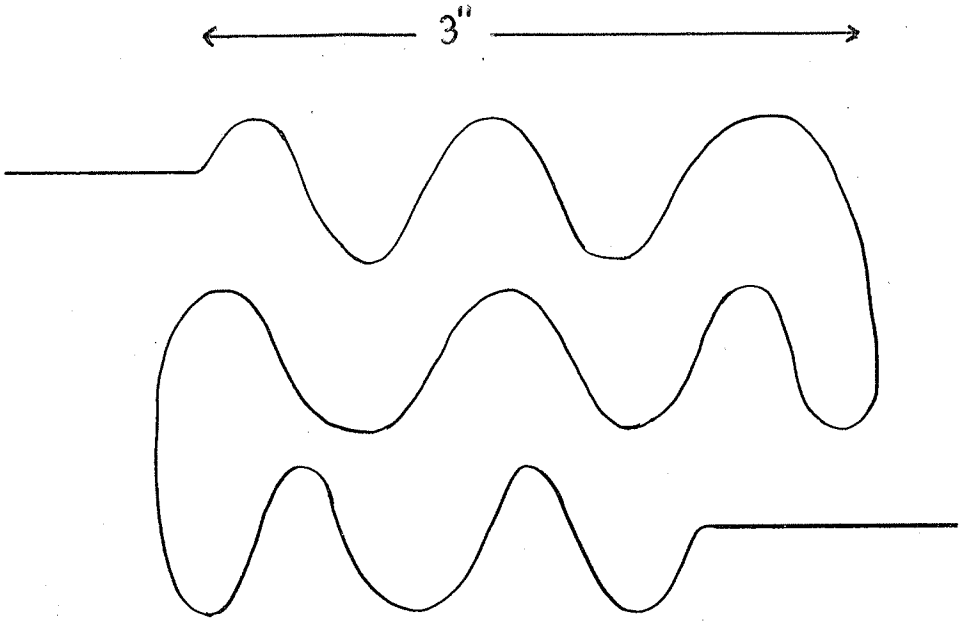

Figure 9. Shape of Filament used for Evaporation

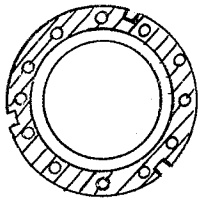

Figure 7. Interferometer Plate Holder

A- liquid air trap
B- german silver tubes
C- water for cooling
D- transformer for current supply to filament
E end window

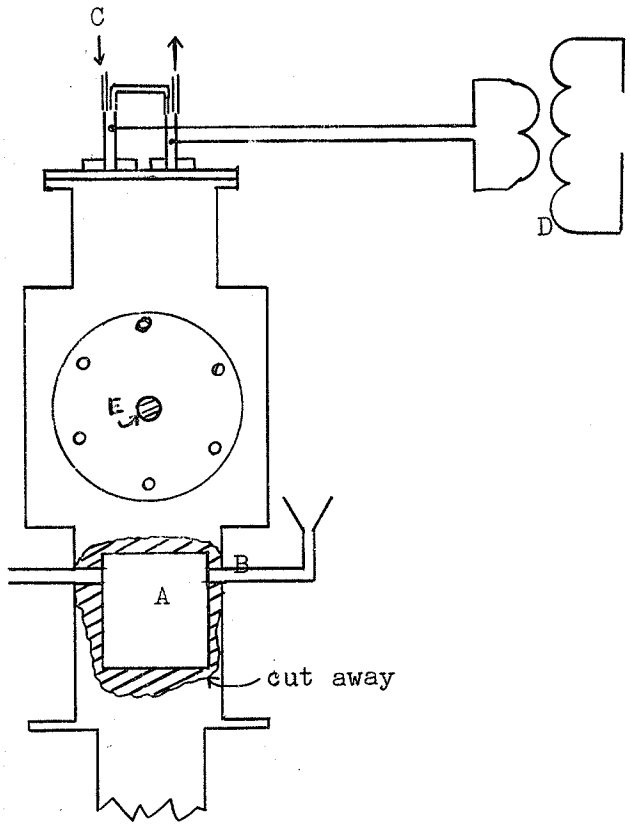

Figure 10. End-on view of Evaporater.